Heritage Science

RESEARCH

Open Access

In-situ non-invasive analysis of conservation materials on mural paintings: a systematic approach in Dahuting Han Dynasty Tomb

Zhuo Wang[1,2,3*], Yaopeng Yin[1,2,3], Zhongwei Shan[1,2,3,4], Qiang Cui[1,2,3], Wenyuan Zhang[1,2,3], Bolong Chai[1,2,3], Dandan Li[1,2,3], Zongren Yu[1,2,3*] and Bomin Su[1,2,3*]

Abstract

In this study, the in-situ non-invasive analysis of the conservation materials on the mural paintings in the Dahuting Han Dynasty Tomb was performed. The analytical process of non-invasive measurement for mural conservation materials has been designed, including digital microscopy, external reflectance Fourier transform infrared spectroscopy, and optical coherence tomography. By using these methods, effective analytical results have been acquired. The microscopic morphologies of the murals were observed and recorded via a portable digital microscope, thereby the effects of the conservation materials on the surface of the murals and the structural characteristics of the coatings were clarified. Through external reflectance Fourier transform infrared spectroscopy analysis, it was found that both the painting ground layer and the edge reinforcement material are calcium carbonate, and there are cellulose nitrate and poly(methyl methacrylate) as conservation materials on the surfaces of the murals in different areas. The spatial location and distribution of these conservation materials were determined by principal component analysis of infrared spectra. The thicknesses of cellulose nitrate and poly(methyl methacrylate) coatings were measured by optical coherence tomography. The above work laid a solid foundation for the subsequent conservation and restoration of the murals. It is proved that the in-situ non-invasive analytical methods applied in this work have broad prospects for the measurement of conservation materials on murals.

Keywords Mural painting, Conservation material, Non-invasive analysis, Fourier transform infrared spectroscopy, Principal component analysis, Optical coherence tomography

Introduction

The Dahuting Han Dynasty Tombs are located in the west of Dahuting Village, Xinmi County, Henan Province, China (Fig. 1a). These tombs are two of the biggest Han Dynasty tombs in China and have over 1800 years of history. The tombs of the east and west are situated side by side. From February to December in 1961, the Institute of Cultural Relics of Henan Province excavated these two tombs. The west tomb, which is numbered Tomb No. 1, has a large number of finely carved stone portraits. The east tomb, which is numbered Tomb No. 2 (Fig. 1b), contains a large quantity of colored and black murals that are of great historical and artistic value. The colored murals are basically well-preserved and distributed on the east,

*Correspondence:
Zhuo Wang
wangzhuo@dha.ac.cn
Zongren Yu
13588975@qq.com
Bomin Su
suboming@hotmail.com
[1] Dunhuang Academy, Dunhuang 736200, People's Republic of China
[2] National Research Center for Conservation of Ancient Wall Paintings and Earthen Sites, Dunhuang 736200, People's Republic of China
[3] Gansu Provincial Research Center for Conservation of Dunhuang Cultural Heritage, Dunhuang 736200, People's Republic of China
[4] Cultural Heritage Conservation and Design Consulting Co., Ltd of Gansu Mogao Grottoes, Dunhuang 736200, People's Republic of China

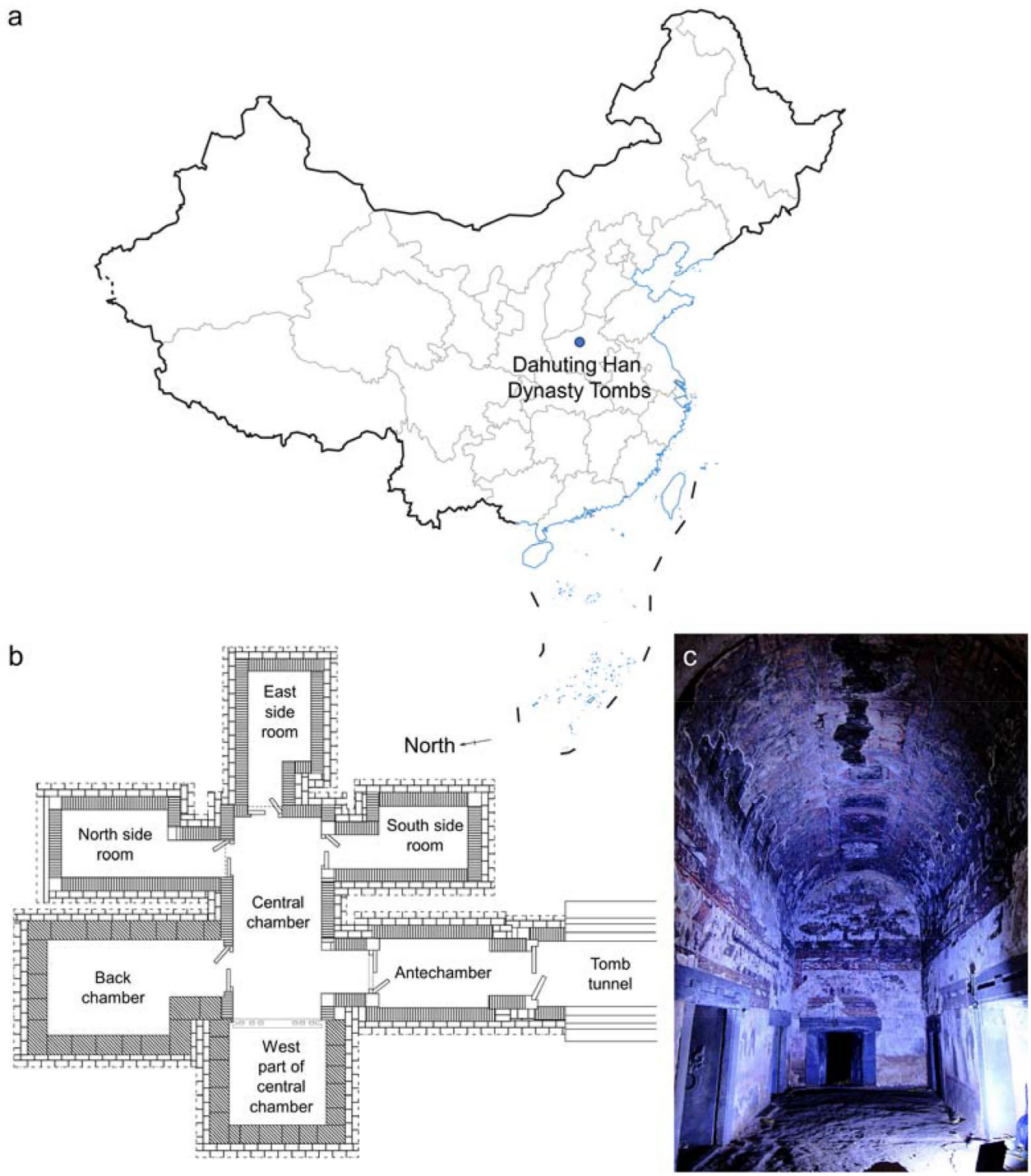

Fig. 1 Brief introduction to Dahuting Han Dynasty Tombs. **a** Location of the tombs in China. **b** Schematic plan of Tomb No. 2. **c** Photograph of the central chamber

south, north walls, and the vaulted ceiling of the central chamber (Fig. 1c). The black murals are mainly observed on the walls of the antechamber and side rooms. The two tombs provide important historical materials for the study of the burial customs, living conditions, and ideology of the middle and upper classes, as well as exquisite artworks of stone carvings and mural paintings in the Eastern Han Dynasty (25–220 A.D.) of China [1].

According to the on-site investigation of Tomb No. 2, we found that the walls of the tomb were made of bricks and coated with lime plaster as a ground layer on which paintings were later painted. The murals appear blurred and illegible owing to the serious coming-off of the lime-whited surfaces on the walls, and many murals have been historically reinforced and restored. But there is no archive available about the compositions of the materials used for conservation. The analysis of the compositions and characteristics of conservation materials is of great significance for evaluating the preservation status of murals and conducting future conservation and restoration.

At present, the conservation materials are typically analyzed by sampling, which may cause slight damage to the murals. The research on non-invasive analytical methods for mural conservation materials has important practical significance. In recent years, various non-invasive analytical techniques for cultural heritages have gradually emerged [2]. These analytical methods have many advantages. Above all, sampling is avoided when determining the surface morphologies and the chemical compositions of cultural relics. Moreover, it is convenient to compare and analyze different areas of the objects. Among all non-invasive analytical techniques, digital microscopy (DM) is the basic method for the preliminary investigation of paintings. The portable DM enables direct observation of the surface of paintings without sampling [3]. The detailed features on the painting surfaces can be carefully observed to provide additional clues for further analysis. External reflectance Fourier transform infrared (ER-FTIR) spectroscopy can obtain the infrared spectra of cultural relics without sampling or contacting. The chemical compositions of organic and inorganic materials on the surfaces of the objects can be elucidated by analyzing the spectral data. This technology has been utilized in many studies of cultural heritages [4], such as oil paintings [5, 6], mural paintings [7–14], modern art materials [15, 16], plastic objects [17–19], stone cultural relics [20, 21], marble artifacts [22], and archaeological burnt bones [23]. In addition, it has been initially applied in the analysis of mural conservation materials on Chinese palace murals [10]. However, the critical difficulty of this technique is the interpretation of obtained spectra. The band shape, position and intensity of ER-FTIR spectra may be distorted by surface roughness and other factors, causing the Reststrahlen effect and derivative shape [4]. In order to interpret the complex spectra acquired, many multivariate statistical methods of chemometrics have been introduced into this field [24, 25]. Among the numerous chemometric tools, principal component analysis (PCA) is a powerful multivariate statistical method used to reduce the complexity of large data sets. Therefore, it can be used to facilitate the interpretation of the spectra and provide visualization of the relationships among spectra [26, 27]. Optical coherence tomography (OCT) is a tomographic imaging technology that uses the Michelson interferometer. OCT can perform non-invasive measurements at depth from several microns to 20 mm below the surfaces of the objects [28]. It has broad application prospects in the non-invasive analysis of cultural heritages [28], such as paintings [29], porcelains [30], and stone objects [31]. The combination of the above methods can form an effective approach to analyze mural conservation materials non-invasively.

Up to now, there are some literatures focused on the composition analysis of frescoes by various non-invasive methods [11–14]. However, there are very few studies specializing in the analysis of conservation materials of mural paintings combining several non-invasive methods [10]. Research in this field is urgently needed. In this study, a general non-invasive analytical process for detecting conservation materials on murals was designed. Non-invasive methods including DM, ER-FTIR spectroscopy, and OCT were used to conduct the comprehensive analysis of the conservation materials on the murals in Dahuting Han Dynasty Tomb No. 2. Eventually, the effective analytical results have laid a solid basis for the subsequent conservation and restoration of the murals.

Materials and methods

In-situ non-invasive analytical process for conservation materials

The general steps of non-invasive analysis of mural conservation materials were shown in Fig. 2. Firstly, microscopic observation of the murals was carried out by DM to determine the microscopic morphologies. Secondly, the chemical compositions of the murals and the

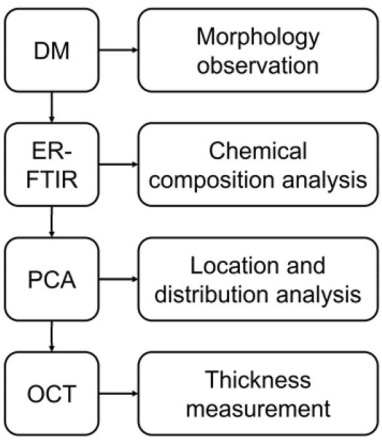

Fig. 2 In-situ non-invasive analytical flow chart for conservation materials

conservation materials on the murals were analyzed by ER-FTIR. Then, the spatial location and distribution of the conservation materials were determined by PCA of ER-FTIR spectra of selected locations. Finally, the thicknesses of the conservation materials were measured by OCT.

Sampling criteria and location of measurements

The integrity and flatness of the murals were taken into consideration in the DM observation and ER-FTIR measurement. OCT measurement was performed on the murals covered with coatings that were analyzed by DM and ER-FTIR. The exact locations of DM observations, ER-FTIR measurements, and OCT measurements were shown in Fig. 3. The height of the measurement points is about 1.5 m from the ground of the tomb.

DM observation

The KEYENCE VHX-600E portable digital microscope was used to observe the microscopic morphologies of the mural surfaces. Lens model: VH-Z20R (20–200×). The micrographs of the murals were obtained by placing the microscope lens on a tripod and recording the images with the instrument's own computer. The size of the image is 1600×1200 pixels and the format of the image is TIFF.

ER-FTIR spectroscopy

The Bruker ALPHA portable FTIR spectrometer was used to study the chemical compositions of murals and conservation materials. The instrument is equipped with an external reflectance module to analyze the murals non-invasively. The ER-FTIR spectra were collected from spot size of about 5 mm in diameter and distance of about 15 mm from the surface of the murals. Measurement parameters are as follows, testing range: 4000 ~ 400 cm^{-1}, spectral resolution: 4 cm^{-1}, number of scans: 128. The spectra were visualized in pseudo-absorbance mode ($A'=\log(1/R)$, R = reflectance). At first, the spectrum of a standard gold-coated mirror was measured as background, and then the flat area of the mural surface was selected for the spectral collection.

PCA of ER-FTIR spectra

The spectral region of PCA was determined between 2000 and 600 cm^{-1} to exclude interferences of systematic noise (600 ~ 400 cm^{-1}) or irrelevant spectral regions. PCA of the spectra was performed using OriginPro 2018, the number of principal components was set to 3. The

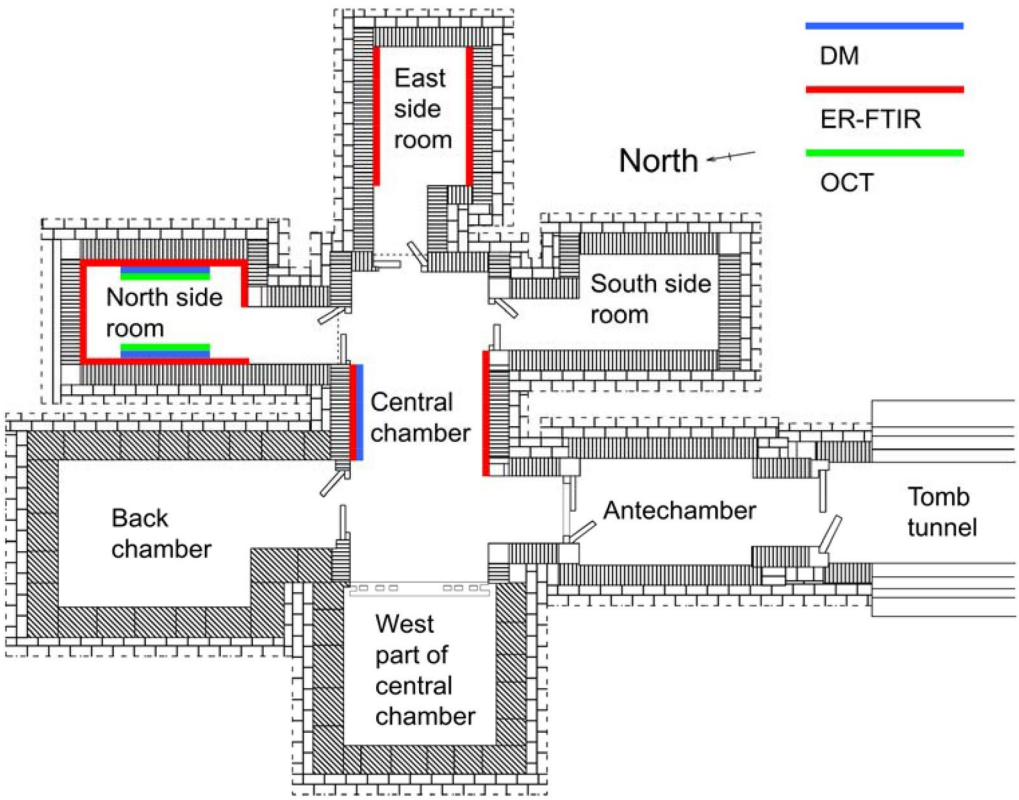

Fig. 3 Exact locations of DM observations, ER-FTIR measurements, and OCT measurements

ER-FTIR spectra of the murals were not subjected to any pre-processing. The total number of spectra for PCA was 43. Considering the integrity of the murals, the measurement points were selected in central chamber, north side room, and east side room. The detailed information of location and number of measurement points were listed in Table 1. The measurement points were almost evenly distributed in the selected areas (Fig. 3), and the spectra were collected once at each measurement point.

OCT measurements

The Thorlabs Ganymede II portable OCT imaging system was used to measure thicknesses of coatings. Instrument parameters are as follows, central wavelength: 900 nm, A-scan rate: 36 kHz, axial resolution: 3.0 μm, imaging depth: 1.9 mm, sensitivity: 93 dB, A-scan max pixels: 1024.

Table 1 Location and number of measurement points in the tomb

Location		Number of points
Central chamber	North wall	5
	South wall	12
East side room	North wall	2
	South wall	6
North side room	North wall	3
	South wall	1
	East wall	8
	West wall	6

Results and discussion

Microscopic observation of mural conservation materials

At first, the in-situ DM was used to get the detailed morphologies of the mural surfaces. By using microphotography, it is possible to observe the details of the mural surfaces from a microscopic perspective. The possible restored areas of the murals can be found. The effects of the conservation materials on the mural surfaces and the morphological characteristics of the coatings can be clarified.

The damaged edge of the mural was reinforced with white solid material, and white beads appeared locally on the reinforcement material. The macrograph (Fig. 4a) shows that the white beads similar to stalactites are attached to the surface of the reinforcement material. The micrograph (Fig. 4b) shows the morphology of the white beads is similar to crystalline aggregate.

The surface of the mural on the north wall in the central chamber exhibits a phenomenon of whitening and flaking. The macrograph (Fig. 4c) shows that there is a white translucent crust covering the surface of the mural. The micrograph (Fig. 4d) shows that the surface of the mural is covered with translucent white waxy substance which is loosely combined with the mural painting layer. In some areas, the white waxy substance leaves the mural surface to form a shell-like suspension or partial detachment. It indicates that the conservation material on the mural surface has been aged [32–34].

There is slight glare on the surface of the murals in other side rooms, and no whitening or flaking phenomenon has been found (Fig. 4e). The micrograph (Fig. 4f) shows that there is a kind of material infiltrating into the

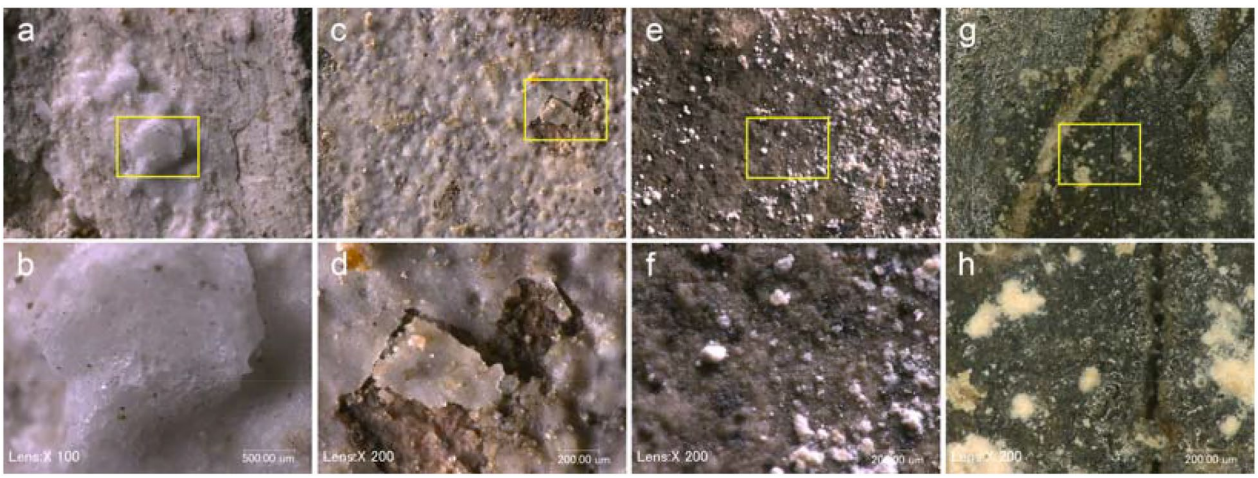

Fig. 4 Macrographs and micrographs of murals, locations of micrographs were indicated by yellow rectangles on macrographs. **a** Macrograph and **b** micrograph (100×) of reinforcement material at the damaged edge. **c** Macrograph and **d** micrograph (200×) of conservation material on north wall in central chamber. **e** Macrograph and **f** micrograph (200×) of conservation material on east wall in north side room. **g** Macrograph and **h** micrograph (200×) of conservation material on west wall in north side room

surface of the mural and it is closely combined with the mural. Referring to our previous work [10], it is speculated that there is a thin layer of conservation material for murals.

Relatively obvious glare phenomenon can be observed on the surface of the mural on the west wall in the north side room. The macrograph (Fig. 4g) shows that the surface of the mural has intense glare. The micrograph (Fig. 4h) shows that there is colorless and transparent substance covering the surface of the mural, which is closely combined with the mural. According to our previous work [10], it is presumed that there is a thick layer of conservation material coating on the surface of the mural.

ER-FTIR analysis of mural conservation materials

By performing ER-FTIR spectroscopy analysis, the chemical compositions of the surface substances and conservation materials of the murals can be revealed, which can provide investigative information for the formulation and implementation of the later conservation and restoration strategies for the murals. The central chamber, east side room and north side room were investigated due to the relatively well-preserved murals in these regions.

Firstly, the ER-FTIR spectroscopy measurement was carried out on the white ground layer of the mural on the north wall in the central chamber, and then the ER-FTIR spectra of the white and black painted surfaces of the murals in the same area were measured respectively. It was found that the testing results of the mural surfaces were the same as the white ground layer. As shown in Fig. 5a, the spectral intensity in the figure is defined as the pseudo-absorbance $A' = \log(1/R)$, where R is the reflectance. In the ER-FTIR spectra, the peak at 2875 cm^{-1} is the overtone band of the asymmetric stretching vibration of carbonate ($2\nu_3$ CO_3^{2-}), the peak at 2512 cm^{-1} along with its shoulder at 2594 cm^{-1} is the combination band of the symmetric and asymmetric stretching vibration of carbonate ($\nu_1+\nu_3$ CO_3^{2-}), the small peak at 1795 cm^{-1} is the combination band of the symmetric stretching and in-plane bending vibrations of carbonate ($\nu_1+\nu_4$ CO_3^{2-}), the minimum at 1410 cm^{-1} is the Reststrahlen band of carbonate asymmetric stretching vibration (ν_3 CO_3^{2-}), the peak at 873 cm^{-1} is out-of-plane bending vibration of carbonate (ν_2 CO_3^{2-}). The above characteristic bands indicate that the ground layer is composed of calcite [22, 35]. ER-FTIR spectra of the white surface and the black painted surface were both demonstrated to be calcite, indicating the murals were made of lime and the black pigment might be carbon (Chinese ink).

Figure 5b shows the ER-FTIR spectra of the white reinforcement material at the damaged edge of the mural on the north wall in the central chamber and white beads on the reinforcement material. The positions of the main bands of the reinforcement material are the same as those of the original ground layer. However, the two peaks around 2981 and 2875 cm^{-1} (overtone and combination bands of the asymmetric stretching vibration of carbonate) are amplified in the spectrum of white beads, while they are not obvious in other spectra. The Reststrahlen band of carbonate asymmetric stretching vibration (ν_3 CO_3^{2-}) at 1500 ~ 1400 cm^{-1} of reinforcement material and white beads is more intense than the ground layer and presents the characteristic inverted shape. The derivative peaks at 873 and 712 cm^{-1} assigned to out-of-plane bending vibration of carbonate (ν_2 CO_3^{2-}) and in-plane bending vibration of carbonate (ν_4 CO_3^{2-}) are

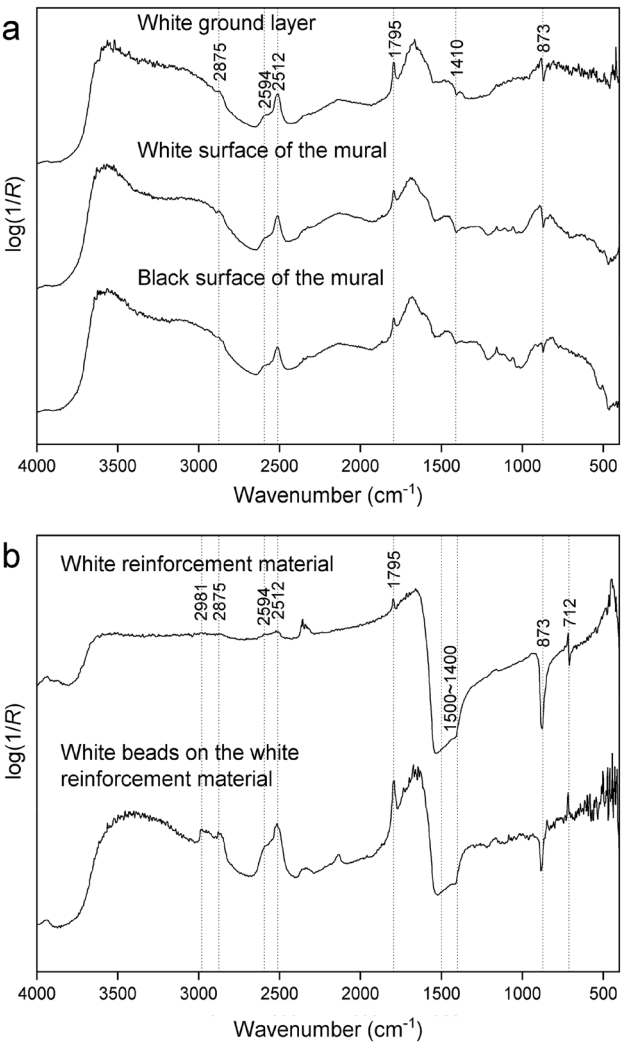

Fig. 5 ER-FTIR spectra of murals on north wall in central chamber. **a** Ground layer and mural surfaces. **b** White reinforcement material and white beads on it (Fig. 4a and b)

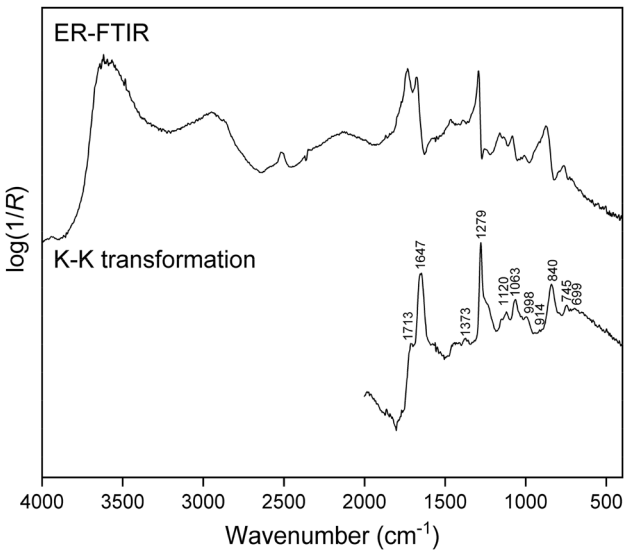

Fig. 6 ER-FTIR and K-K transformation spectra of CN

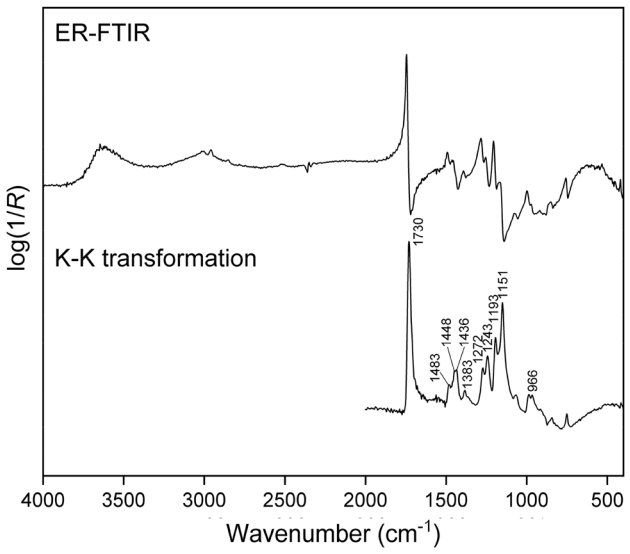

Fig. 7 ER-FTIR and K-K transformation spectra of PMMA

Table 2 Absorption bands and assignments of CN

K-K transformation spectrum (cm^{-1})	Reference spectrum (cm^{-1}) [41, 44]	Δν (cm^{-1})	Assignments
1713	1720	7	C═O stretching
1647	1650	3	NO_2 stretching
1373	1378	5	CH deformation
1279	1280	1	NO_2 stretching
1120	1117	3	C—O stretching
1063	1061	2	C—O stretching
998	1001	3	C—O stretching
914	917	3	CH out-of-plane
840	840	0	N—O stretching
745	747	2	NO_2 wagging
699	692	7	NO_2 scissoring

Table 3 Absorption bands and assignments of PMMA

K-K transformation spectrum (cm^{-1})	Reference spectrum (cm^{-1}) [46]	Δν (cm^{-1})	Assignments
1730	1729	1	C═O stretching
1483	1485	2	CH_2 bending
1448	1450	2	O—CH_3 bending
1436	1434	2	O—CH_3 bending
1383	1382	1	C—CH_3 bending
1272	1265	7	C—O—C stretching
1243	1238	5	C—O—C stretching
1193	1189	4	C—O—C stretching
966	962	4	C—CH_3 bending

visible only in the spectra of reinforcement material and white beads and hardly recognized on the original ground layer. These phenomena are mainly due to the different surface roughness of the reinforcement material, white beads, and original ground layer (Fig. 4a) [22, 35]. The components of the reinforcement material and the white beads on it were both confirmed as calcium carbonate. It is speculated that the edge reinforcement material underwent a corrosion process in the high-humidity environment in the tomb. The formation of the white beads is similar to the formation of stalactites [36–39]. The first step is dissolution. In this step, the surface of the water film on $CaCO_3$ is in direct contact with the atmosphere and CO_2 flows into the solution. $CaCO_3$ combines with H_2O and CO_2 to form $Ca(HCO_3)_2$ which is soluble in water. The second step is precipitation. In this step, carbonate in the solution might become supersaturated due to CO_2 degassing when a drop of water containing $Ca(HCO_3)_2$ contacts the surface of white reinforcement material and a thin film of water spreads out. Calcite is precipitated in a thin layer around the contacting area, resulting in the formation of bead-like calcite crystalline aggregate (Fig. 4b).

The ER-FTIR spectrum of the whitening mural on the north wall in the central chamber was shown in Fig. 6. The spectral region below 2000 cm^{-1} is different from calcite and exhibits derivative-like shape that is mainly due to specular reflection caused by the relatively smooth surface of the coating, which is consistent with the microscopic image of the surface (Fig. 4d). Since the spectrum below 2000 cm^{-1} is not disturbed by the mural

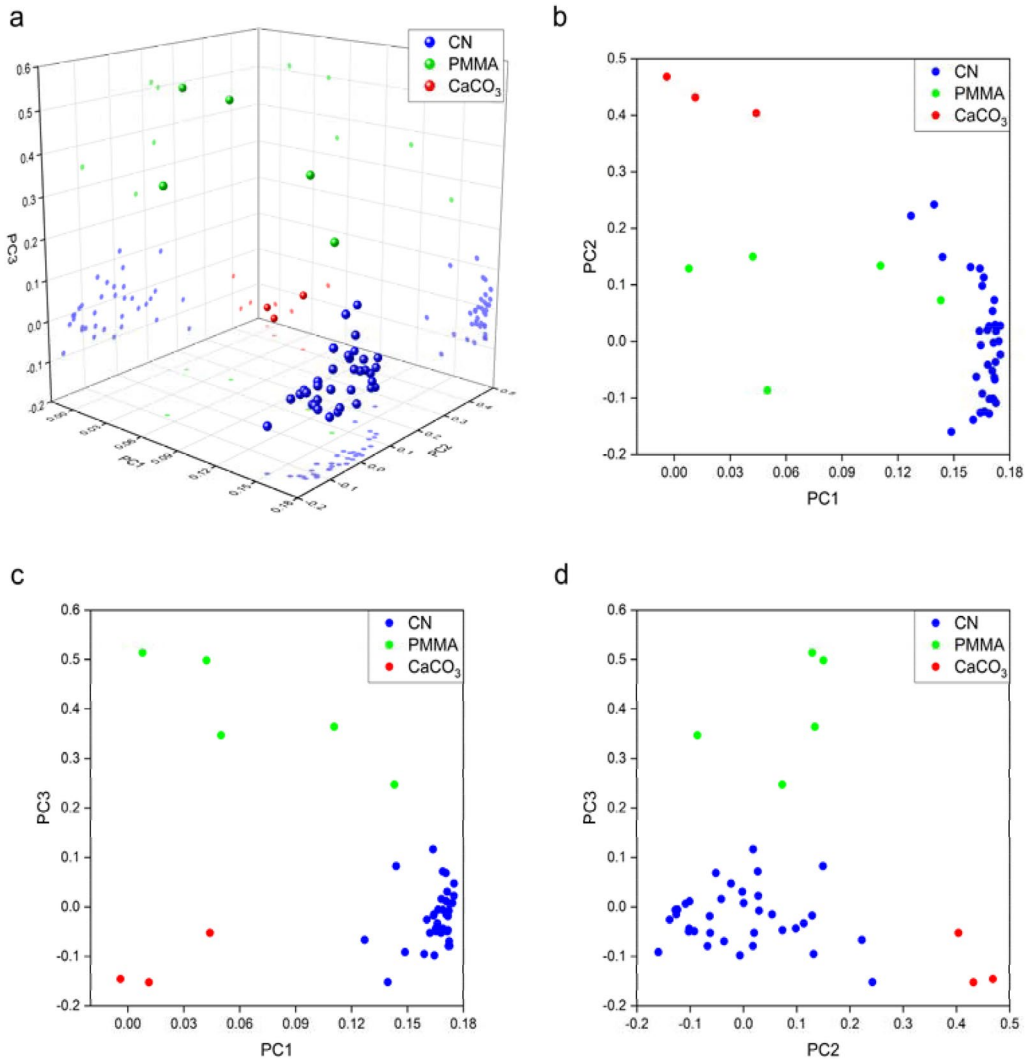

Fig. 8 Score plots of PCA. **a** Score plots of PC1, PC2, PC3. **b** Projection on PC1-PC2 plane. **c** Projection on PC1-PC3 plane. **d** Projection on PC2-PC3 plane

ground layer and contains the fingerprint region of the polymer material, the Kramers–Kronig (K-K) transformation was performed on the 2000 ~ 400 cm^{-1} region [10]. As the K-K transformation spectrum shown in Fig. 6, the peak at 1647 cm^{-1} is assigned to the asymmetric stretching vibration of NO_2, the peak at 1279 cm^{-1} is assigned to the symmetric stretching vibration of NO_2, and the peak at 840 cm^{-1} is N—O stretching vibration. The band near 1063 cm^{-1} is the characteristic band of cellulose. All the bands are the characteristic bands of cellulose nitrate (CN) [40]. The peak at 1713 cm^{-1} assigned to the C═O stretching vibration may indicate the aging of CN [41]. The coating on the mural is determined to be CN which is presumed to be one kind of material for historical conservation. The difference of the absorption bands between the K-K transformation spectrum and the reference spectrum (Δν), and the detailed spectral assignments were listed in Table 2. The maximal Δν is 7 cm^{-1}, indicating the effectiveness of K-K transformation as a data processing method. As far as we know, CN is rarely used in mural conservation, but it is usually used as an adhesive for pottery [40] and film base [42, 43]. The murals in Dahuting Han Dynasty Tomb No. 2 were reinforced in the 1960s after the excavation. At that time, there were few materials available for mural conservation in wet environments in China. CN was relatively easy to obtain, so the restorers employed it to reinforce the murals.

The ER-FTIR spectrum of the glare mural on the west wall in the north side room was shown in Fig. 7. The

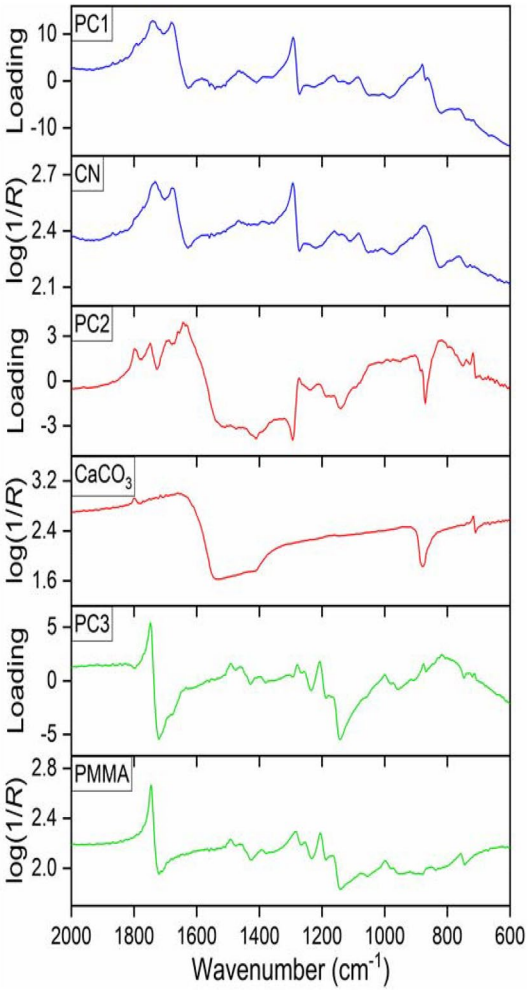

Fig. 9 Loading plots of PC1, PC2, PC3 and ER-FTIR spectra of CN, $CaCO_3$, PMMA

spectrum below 2000 cm^{-1} is different from calcite. Meanwhile, this part of the spectrum shows derivative-like shape due to specular reflection caused by the smooth surface shown in the microscopic image (Fig. 4h). K-K transformation was also carried out in the region of 2000 ~ 400 cm^{-1}. As shown in Fig. 7, the peak at 1730 cm^{-1} is C═O stretching vibration, the peak at 1483 cm^{-1} is CH_2 bending vibration, the peaks at 1448 and 1436 cm^{-1} are O—CH_3 bending vibration, and the peak at 1383 cm^{-1} is C—CH_3 bending vibration. The splitting peaks at 1272 and 1243 cm^{-1} are C—O—C asymmetric stretching vibration, and the splitting peaks at 1193 and 1151 cm^{-1} are C—O—C symmetric stretching vibration. The splitting of C—O—C stretching vibration is the structural characteristic of polymethacrylate. The spectrum has all the characteristics of poly(methyl methacrylate) (PMMA) [45]. As shown in Table 3, the maximal Δν is 7 cm^{-1}, indicating the K-K transformation in the data processing is also effective. It is concluded that PMMA is another kind of historical conservation material.

PCA of ER-FTIR spectra

The principle of PCA is to replace complex multidimensional spectral data by a series of simplified components with fewer dimensions named principal components while retaining most of the characteristic information of the original variables [47]. It is very suitable for distinguishing complex infrared spectra of different conservation materials. The rules of selecting spectral regions depend on the distinguishable characteristic absorption bands of all the compounds [48]. In order to improve the PCA results, the wavenumber range between 2000 and 600 cm^{-1} was taken into consideration to exclude interferences of systematic noise (600 ~ 400 cm^{-1}) or irrelevant spectral regions. Additionally, the fingerprint regions of CN, PMMA, and $CaCO_3$ are included in this region very well.

The scores of principal components indicate the amount of variance explained by each principal component (PC). In this study, three PCs were considered during PCA modeling. The first three PCs totally explained 87.88% of the total variance, where PC1, PC2, and PC3 captured 66.05%, 13.87%, and 7.96%, respectively. The first component (PC1) is the most important one due to its highest variance percentage. The score plots of PC1, PC2, and PC3 were presented in Fig. 8a along with their projections on PC1-PC2 plane (Fig. 8b), PC1-PC3 plane (Fig. 8c), and PC2-PC3 plane (Fig. 8d). The visual presentation of the PCA data displays the existence of distinct grouping structure and clear separation. The projections of PCs could further enhance the visual discrimination. As shown in Fig. 8, the coefficient of CN on PC1 is 0.12 ~ 0.18, the coefficient of $CaCO_3$ on PC2 is 0.4 ~ 0.5, and the coefficient of PMMA on PC3 is 0.2 ~ 0.6, indicating that CN, $CaCO_3$, and PMMA are positively related to PC1, PC2, and PC3 respectively within our experiments.

Loading plot for each PC indicate the degree to which each wavenumber contributes to the variance explained by that particular PC [26, 40]. In short, it reflects the correlation between a PC and a variable. Loading plots were stacked onto the ER-FTIR spectra of CN, $CaCO_3$, and PMMA to identify correlations between PCs and spectra. The correlations were found subsequently. As shown in Fig. 9, the loading plots of PC1, PC2, and PC3 were positively correlated with the spectra of CN, $CaCO_3$, and PMMA respectively, which is consistent with the score plots (Fig. 8). The above results indicate that the ER-FTIR

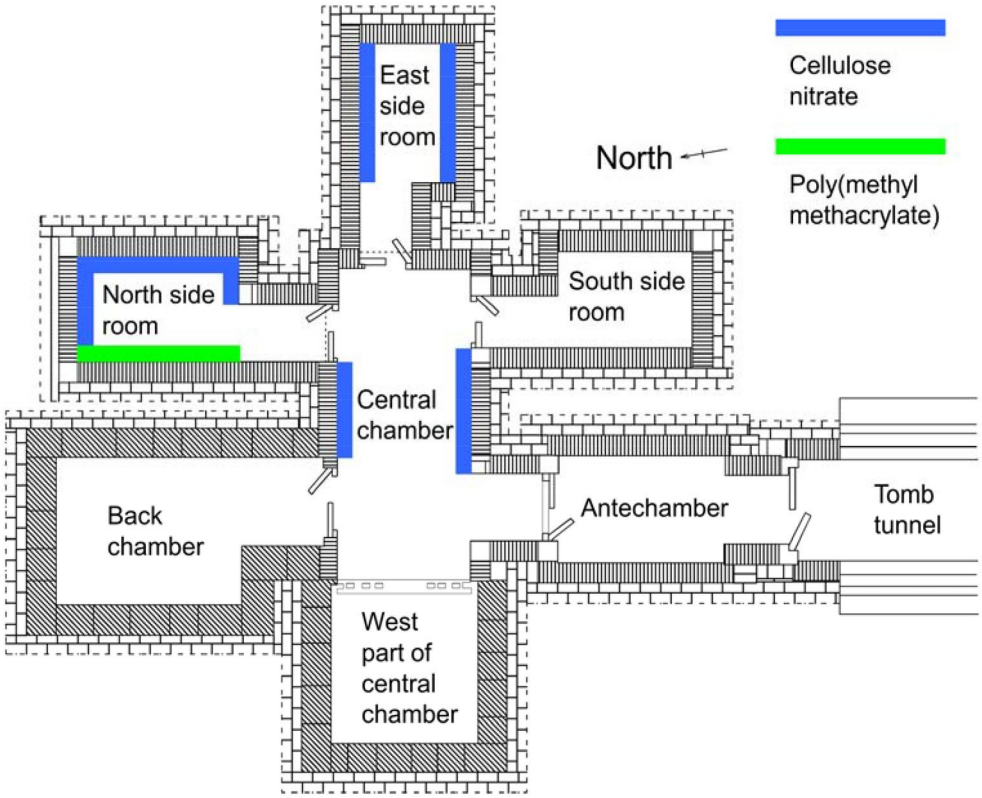

Fig. 10 Spatial location and distribution of conservation materials on murals

spectra of these materials could be successfully distinguished by PCA.

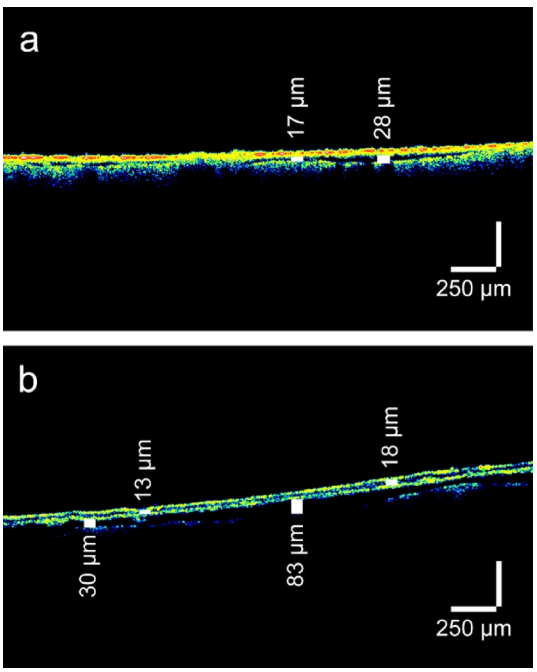

Fig. 11 OCT images of conservation materials. **a** CN. **b** PMMA

After the conducting of PCA of ER-FTIR spectra, a map of the spatial location and distribution of the conservation materials on the murals in Dahuting Han Dynasty Tomb No. 2 was drawn. As shown in Fig. 10, the conservation material on the west wall in the north side room is PMMA, the conservation material on other areas is CN.

OCT measurement of mural conservation materials

In order to get a deeper understanding of the reasons for the glare phenomena caused by conservation materials on the murals, the in-situ OCT technique was used to measure the thicknesses of the coatings. In this study, OCT measurement was carried out on the east and west walls in the north side room. As shown in Fig. 11a, the thickness of the conservation material CN on the east wall in the north side room was measured to be 17 ~ 28 μm. The thickness of the film is thin and the distribution of the film is not uniform, so it looks like a layer of translucent white waxy substance, which is consistent with the microscopic observation (Fig. 4f). As shown in Fig. 11b, the conservation material PMMA on the west wall in the north side room is partially divided into two layers, which may be caused by repeated brushing. The thicknesses are 13 ~ 18 μm and 30 ~ 83 μm for the upper layer and lower layer, respectively. PMMA is smoother

and thicker than CN, resulting in a severe glare phenomenon shown in the micrograph (Fig. 4h).

Conclusion

In this study, in-situ non-invasive analysis of the mural conservation materials in Dahuting Han Dynasty Tomb No. 2 was carried out by applying DM, ER-FTIR spectroscopy, and OCT. The surface details of the murals were observed by microphotography using in-situ DM. By this way, the morphologies of the conservation materials were discussed and the structural characteristics of the coatings were clarified. The following conclusions can be drawn from ER-FTIR analysis. The mural ground layer is composed of calcite. Both the white reinforcement material and white beads on it at the damaged edge of the murals are calcium carbonate. Two kinds of organic conversation materials were found on the surfaces of the murals. One is CN and another is PMMA. It is proved that ER-FTIR spectroscopy can obtain reliable results in the tomb environment with high humidity. The classification of the ER-FTIR spectra was conducted by using PCA. Then, a map of the spatial location and distribution of the conservation materials on the murals in Dahuting Han Dynasty Tomb No. 2 was drawn. The thicknesses of CN and PMMA coatings were measured by OCT, which explained the cause of the glare phenomena on the mural surfaces. The integrated non-invasive methods formed an in-situ analytical process for measuring mural conservation materials. By executing the above process, comprehensive analytical results of mural conservation materials could be obtained. The analytical results can provide significant reference for the removal of the mural conservation materials and laid a solid foundation for the subsequent conservation and restoration in the future. The systematic approach in this study provides broad application prospects for research in analyzing mural conservation materials.

Abbreviations

DM	Digital microscopy
ER-FTIR	External reflectance Fourier transform infrared
PCA	Principal component analysis
OCT	Optical coherence tomography
K-K	Kramers–Kronig
CN	Cellulose nitrate
PMMA	Poly(methyl methacrylate)
PC	Principal component

Acknowledgements

It is a great honor to have the opportunity to investigate the mural paintings in Dahuting Han Dynasty Tomb. We are very grateful to the managers of this cultural heritage who facilitated our work. I am very thankful to my colleagues for their help in this work. The authors would like to thank the editors and reviewers for providing valuable comments.

Author contributions

BMS, ZRY and WYZ provided support and guidance for this study. ZW performed ER-FTIR measurement and PCA and prepared the manuscript. YPY performed OCT measurement. ZWS and QC performed DM measurement. BLC performed photography. DDL performed schematic plan drawing. All authors read and approved the final manuscript.

Funding

This research was supported by National Key Research and Development Program of China (2019YFC1520700, 2019YFC1520100), National Natural Science Foundation of China (U21A20282, 12204103, 51962001), the Natural Science Foundation of Gansu Province (22JR5RA800), the Local Project Guided by the Central Government of Gansu Province (YDZX20216200001728), Longyuan Youth Innovation and Entrepreneurship Talent Project of Gansu Province (2020RCXM150).

Availability of data and materials

All data and materials in this study are included in this published article.

Declarations

Competing interests

The authors declare that they have no competing interests.

Received: 28 September 2023 Accepted: 30 January 2024
Published online: 13 February 2024

References

1. The Henan Provincial Institute of Archaeology. Han dynasty tombs at Dahuting village in Mixian county. Beijing: Cultural Relics Publishing House; 1993.
2. Miliani C, Rosi F, Brunetti BG, Sgamellotti A. In situ noninvasive study of artworks: the MOLAB multitechnique approach. Acc Chem Res. 2010;43:728–38.
3. Galli A, Caccia M, Bonizzoni L, Gargano M, Ludwig N, Poldi G, Martini M. Deep inside the color: how optical microscopy contributes to the elemental characterization of a painting. Microchem J. 2020;155:104730.
4. Izzo F, Germinario C, Grifa C, Langella A, Mercurio M. External reflectance FTIR dataset (4000–400 cm^{-1}) for the identification of relevant mineralogical phases forming cultural heritage materials. Infrared Phys Techn. 2020;106:103266.
5. Manfredi M, Barberis E, Rava A, Robotti E, Gosetti F, Marengo E. Portable diffuse reflectance infrared Fourier transform (DRIFT) technique for the non-invasive identification of canvas ground: IR spectra reference collection. Anal Methods. 2015;7:2313–22.
6. Miliani C, Rosi F, Burnstock A, Brunetti BG, Sgamellotti A. Non-invasive in-situ investigations versus micro-sampling: a comparative study on a Renoirs painting. Appl Phys A. 2007;89:849–56.
7. Miliani C, Rosi F, Borgia I, Benedetti P, Brunetti BG, Sgamellotti A. Fiber-optic Fourier transform mid-infrared reflectance spectroscopy: a suitable technique for in situ studies of mural paintings. Appl Spectrosc. 2007;61:293–9.
8. Rosi F, Daveri A, Miliani C, Verri G, Benedetti P, Piqué F, Brunetti BG, Sgamellotti A. Non-invasive identification of organic materials in wall paintings by fiber optic reflectance infrared spectroscopy: a statistical multivariate approach. Anal Bioanal Chem. 2009;395:2097–106.
9. Al-Emam E, Motawea AG, Janssens K, Caen J. Evaluation of polyvinyl alcohol–borax/agarose (PVA–B/AG) blend hydrogels for removal of deteriorated consolidants from ancient Egyptian wall paintings. Herit Sci. 2019;7:22.
10. Wang Z, Su BM, Yu ZR, Shui BW, Zhao JL, Cui Q, Shan ZW, Li Q. In-situ non-invasive FTIR analysis of conservation materials on the surface of mural paintings in prince Shi's palace of the Taiping heavenly kingdom. Spectrosc Spect Anal. 2020;40:356–61.
11. Alberghina MF, Germinario C, Bartolozzi G, Bracci S, Grifa C, Izzo F, La Russa MF, Magrini D, Massa E, Mercurio M, Nardo VM, Oddo ME, Pagnotta SM, Pelagotti A, Ponterio RC, Ricci P, Rovella N, Ruffolo SA, Schiavone S,

Spagnuolo A, Vetromile C, Zuchtriegel G, Lubritto C. The tomb of the diver and the frescoed tombs in Paestum (southern Italy): new insights from a comparative archaeometric study. PLoS ONE. 2020;15:e0232375.
12. Galli A, Alberghina MF, Re A, Magrini D, Grifa C, Ponterio RC, La Russa MF. Special issue: results of the II national research project of AIAr archaeometric study of the frescoes by Saturnino Gatti and workshop at the church of San Panfilo in Tornimparte (AQ, Italy). Appl Sci-Basel. 2023;13:8924.
13. Madariaga JM, Maguregui M, Castro K, Knuutinen U, Martínez-Arkarazo I. Portable raman, DRIFTS, and XRF analysis to diagnose the conservation state of two wall painting panels from pompeii deposited in the naples national archaeological museum (Italy). Appl Spectrosc. 2016;70:137–46.
14. Germinario C, Francesco I, Mercurio M, Langella A, Sali D, Kakoulli I, De Bonis A, Grifa C. Multi-analytical and non-invasive characterization of the polychromy of wall paintings at the Domus of Octavius Quartio in Pompeii. Eur Phys J Plus. 2018;133:359.
15. Rosi F, Miliani C, Clementi C, Kahrim K, Presciutti F, Vagnini M, Manuali V, Daveri A, Cartechini L, Brunetti BG, Sgamellotti A. An integrated spectroscopic approach for the non-invasive study of modern art materials and techniques. Appl Phys A-Mater. 2010;100:613–24.
16. Rosi F, Burnstock A, Van den Berg KJ, Miliani C, Brunetti BG, Sgamellotti A. A non-invasive XRF study supported by multivariate statistical analysis and reflectance FTIR to assess the composition of modern painting materials. Spectrochim Acta A Mol Biomol Spectrosc. 2009;71:1655–62.
17. Bell J, Nel P, Stuart B. Non-invasive identification of polymers in cultural heritage collections: evaluation, optimisation and application of portable FTIR (ATR and external reflectance) spectroscopy to three-dimensional polymer-based objects. Herit Sci. 2019;7:95.
18. Soares I, de Sa SF, Ferreira JL. A first approach into the characterisation of historical plastic objects by in situ diffuse reflection infrared fourier transform (DRIFT) spectroscopy. Spectrochim Acta A Mol Biomol Spectrosc. 2020;240:118548.
19. Saviello D, Toniolo L, Goidanich S, Casadio F. Non-invasive identification of plastic materials in museum collections with portable FTIR reflectance spectroscopy: Reference database and practical applications. Microchem J. 2016;124:868–77.
20. Delgado Robles AA, Ruvalcaba Sil JL, Claes P, Manrique Ortega MD, Casanova González E, Maynez Rojas MÁ, Cuevas García M, García CS. Non-destructive in situ spectroscopic analysis of greenstone objects from royal burial offerings of the Mayan site of Palenque. Mexico Herit Sci. 2015;3:20.
21. Prinsloo LC, Wadley L, Lombard M. Infrared reflectance spectroscopy as an analytical technique for the study of residues on stone tools: potential and challenges. J Archaeol Sci. 2014;41:732–9.
22. Ricci C, Miliani C, Brunetti BG, Sgamellotti A. Non-invasive identification of surface materials on marble artifacts with fiber optic mid-FTIR reflectance spectroscopy. Talanta. 2006;69:1221–6.
23. Legan L, Leskovar T, Cresnar M, Cavalli F, Innocenti D, Ropret P. Non-invasive reflection FTIR characterization of archaeological burnt bones: reference database and case studies. J Cult Herit. 2020;41:13–26.
24. Manfredi M, Barberis E, Aceto M, Marengo E. Non-invasive characterization of colorants by portable diffuse reflectance infrared fourier transform (DRIFT) spectroscopy and chemometrics. Spectrochim Acta A Mol Biomol Spectrosc. 2017;181:171–9.
25. Sessa C, Bagan H, Garcia JF. Influence of composition and roughness on the pigment mapping of paintings using mid-infrared fiberoptics reflectance spectroscopy (mid-IR FORS) and multivariate calibration. Anal Bioanal Chem. 2014;406:6735–47.
26. Nel P, Lonetti C, Lau D, Tam K, Sagona A, Sloggett RS. Analysis of adhesives used on the Melbourne University Cypriot pottery collection using a portable FTIR-ATR analyzer. Vib Spectrosc. 2010;53:64–70.
27. Navas N, Romero-Pastor J, Manzanoa E, Cardell C. Benefits of applying combined diffuse reflectance FTIR spectroscopy and principal component analysis for the study of blue tempera historical painting. Anal Chim Acta. 2008;630:141–9.
28. Targowski P, Iwanicka M. Optical coherence tomography: its role in the non-invasive structural examination and conservation of cultural heritage objects-a review. Appl Phys A-Mater. 2012;106:265–77.
29. Iwanicka M, Vlachou-Mogire C, Pereira-Pardo L, Sylwestrzak M, Kowalska M, Targowski P. Non-invasive survey of Rubens' ceiling paintings at the banqueting house whitehall, London, by means of optical coherence tomography. Stud Conserv. 2022;67:161–7.
30. Targowski P, Rouba B, Wojtkowski M, Kowalczyk A. The application of optical coherence tomography to non-destructive examination of museum objects. Stud Conserv. 2004;49:107–14.
31. Yang ML, Lu CW, Hsu IJ, Yang CC. The use of optical coherence tomography for monitoring the subsurface morphologies of archaic jades. Archaeometry. 2004;46:171–82.
32. Quye A, Littlejohn D, Pethrick RA, Stewart RA. Accelerated ageing to study the degradation of cellulose nitrate museum artefacts. Polym Degrad Stabil. 2011;96:1934–9.
33. Quye A, Littlejohn D, Pethrick RA, Stewart RA. Investigation of inherent degradation in cellulose nitrate museum artefacts. Polym Degrad Stabil. 2011;96:1369–76.
34. Edge M, Allen NS, Hayes M, Riley PNK, Horie CV, Lucgardette J. Mechanisms of deterioration in cellulose nitrate base archival cinematograph film. Eur Polym J. 1990;26:623–30.
35. Brunello V, Corti C, Sansonetti A, Tedeschi C, Rampazzi L. Non-invasive FTIR study of mortar model samples: comparison among innovative and traditional techniques. Eur Phys J Plus. 2019;134:270.
36. Buhmann D, Dreybrodt W. The kinetics of calcite dissolution and precipitation in geologically relevant situations of karst areas.1. Open system. Chem Geol. 1985;8:189–211.
37. Buhmann D, Dreybrodt W. The kinetics of calcite dissolution and precipitation in geologically relevant situations of karst areas. 2. Closed system. Chem Geol. 1985;53:109–24.
38. Short MB, Baygents JC, Beck JW, Stone DA, Toomey RS, Goldstein RE. Stalactite growth as a free-boundary problem: a geometric law and its platonic ideal. Phys Rev Lett. 2005;94:018501.
39. Short MB, Baygents JC, Goldstein RE. Stalactite growth as a free-boundary problem. Phys Fluids. 2005;17:083101.
40. Noake E, Lau D, Nel P. Identification of cellulose nitrate based adhesive repairs in archaeological pottery of the University of Melbourne's Middle Eastern archaeological pottery collection using portable FTIR-ATR spectroscopy and PCA. Herit Sci. 2017;5:3.
41. Shashoua Y, Bradley SM, Daniels VD. Degradation of cellulose nitrate adhesive. Stud Conserv. 1992;37:113–9.
42. Nunes S, Ramacciotti F, Neves A, Angelin EM, Ramos AM, Roldao E, Wallaszkovits N, Armijo AA, Melo MJ. A diagnostic tool for assessing the conservation condition of cellulose nitrate and acetate in heritage collections: quantifying the degree of substitution by infrared spectroscopy. Herit Sci. 2020;8:33.
43. Carter EA, Swarbrick B, Harrison TM, Ronai L. Rapid identification of cellulose nitrate and cellulose acetate film in historic photograph collections. Herit Sci. 2020;8:51.
44. Kovalenko VI, Mukhamadeeva RM, Maklakova LN, Gustova NG. Interpretation of the IR-spectrum and structure of cellulose nitrate. J Struct Chem. 1993;34:540–7.
45. Huth F, Govyadinov A, Amarie S, Nuansing W, Keilmann F, Hillenbrand R. Nano-FTIR absorption spectroscopy of molecular fingerprints at 20 nm spatial resolution. Nano Lett. 2012;12:3973–8.
46. Stuart BH. Infrared spectroscopy: fundamentals and applications. New York: Wiley; 2004.
47. Sessa C, Bagan H, Garcia JF. Evaluation of MidIR fibre optic reflectance: detection limit, reproducibility and binary mixture discrimination. Spectrochim Acta A Mol Biomol Spectrosc. 2013;115:617–28.
48. Sarmiento A, Perez-Alonso M, Olivares M, Castro K, Martinez-Arkarazo I, Fernandez LA, Madariaga JM. Classification and identification of organic binding media in artworks by means of Fourier transform infrared spectroscopy and principal component analysis. Anal Bioanal Chem. 2011;399:3601–11.

Publisher's Note